Multiresonant Feedback Control of a Three-Degree-of-Freedom Wave Energy Converter

Ossama Abdelkhalik, Shangyan Zou, Rush D. Robinett, III, Giorgio Bacelli, David G. Wilson, *Senior Member, IEEE*, Ryan Coe, and Umesh Korde

***Abstract*—For a three-degree-of-freedom wave energy converter (heave, pitch, and surge), the equations of motion could be coupled depending on the buoy shape. This paper presents a multiresonant feedback control, in a general framework, for this type of a wave energy converter that is modeled by linear time invariant dynamic systems. The proposed control strategy finds the optimal control in the sense that it computes the control based on the complex conjugate criteria. This control strategy is relatively easy to implement since it is a feedback control in the time domain that requires only measurements of the buoy motion. Numerical tests are presented for two different buoy shapes: a sphere and a cylinder. Regular, Bretschnieder, and Ochi–Hubble waves are tested. Simulation results show that the proposed controller harvests energy in the pitch-surge-heave modes that is about three times the energy that can be harvested using a heave-only device. This multiresonant control can also be used to shift the energy harvesting between the coupled modes, which can be exploited to eliminate one of the actuators while maintaining about the same level of energy harvesting.**

***Index Terms*—Multi resonant control, three degrees of freedom WEC, wave energy conversion.**

I. Introduction

RENEWABLE energy continues to receive more interest because of the growing energy needs and the limitations associated with classical energy sources in terms of environmental effects and the available reserves. Wave energy is one of the renewable sources that has great potential yet to be utilized. One of the main reasons why wave energy is not in a fully commercial state yet is the absence of economic design of a Wave Energy Converter (WEC). Most of the existing studies in wave energy focus on single Degree-Of-Freedom (DOF) WECs, such as the studies in [1]–[5]. There is a variety of methods for heave control that range from controls that do not need reactive power, such as the resistive control [6] and latching [7], [8], to more complex methods that require an actuator with the capability to provide reactive power. Of particular importance among the different control strategies is the well known complex conjugate control (C3). The complex conjugate control criteria is two folds. First, it resonates the system natural frequencies with the frequencies of the wave excitation force. Second, it adds damping that is equal in magnitude to the system's damping at each frequency. This C3 criteria is shown to guarantee optimal energy harvesting in heave motion [9]. The implementation of the C3 criteria, however, has its own challenges; of them is the need to know the frequencies of the wave excitation force. This motivates the wave by wave control approach [10], in which the up-wave elevation measurements are needed [11]. Other studies have investigated the use of relative motion of multiple bodies in a heave mode [4], [12]. Reference [13], for instance, presented a sensitivity analysis for a three-body heave WEC to examine how the characteristics of the heave plate and the component masses affect the performance of the system, and concluded that the system is dominated by inertia more than drag.

The main reason for the focus on single DOF WECs is the complexity of designing multiple DOF actuators in addition to the complexity of the control logic itself. On the other hand, other references motivate the use of a multiple-DOF WEC as opposed to a single mode WEC [14]. Reference [15] extended the results of two dimensional WECs to bodies in channels and accounts for the effect of body orientation on the energy harvesting. In fact reference [16] points out that the power that can be extracted from a mode that is antisymmetric to the wave (such as pitch and surge) is twice as much that can be extracted from a mode that is symmetric (such as heave). Reference [16] also points out that roll, yaw, and sway modes are not coupled to the wave and hence concludes that the pitch and surge motions are the most attractive power conversion modes. Moreover, the reactive power in the pitch and surge modes was less than that in the heave for the frog system proposed in [16]. Reference [17] investigated experimentally the performance of a surge-heave-pitch WEC for the Edinburgh Duck, on a rig that allowed the duck to move in the 3-DOF. The controller in this experiment optimized the spring and damping coefficients in each of the

Manuscript received October 14, 2016; revised January 16, 2016 and March 9, 2017; accepted April 4, 2017. Date of publication April 12, 2017; date of current version September 15, 2017. This work was supported by the Advanced WEC Control Project at Sandia National Laboratories (Sandia National Laboratories is a multi-program laboratory managed and operated by Sandia Corporation, a wholly owned subsidiary of Lockheed Martin Corporation, for the U.S. Department of Energys National Nuclear Security Administration under contract DE-AC04-94AL85000). The advanced WEC control project at Sandia National Laboratory was supported by the Department of Energy, Office of Energy Efficiency and Renewable Energy, Wind and Water Power Technologies Office. Paper no. TSTE-00790-2016. *(Corresponding author: Ossama Abdelkhalik.)*

O. Abdelkhalik, S. Zou, R.D. Robinett, and U. Korde are with the Department of Mechanical Engineering–Engineering Mechanics, Michigan Technological University, Houghton, MI 49931 USA (e-mail: ooabdelk@mtu.edu; szou2@mtu.edu; rdrobine@mtu.edu; uakorde@mtu.edu).

G. Bacelli, D. G. Wilson, and R. Coe are with Sandia National Laboratory, Albuquerque, NM 87185 USA (e-mail: gbacell@sandia.gov; dwilso@sandia.gov).

Color versions of one or more of the figures in this paper are available online at http://ieeexplore.ieee.org.

Digital Object Identifier 10.1109/TSTE.2017.2692647

three modes, in addition to the product of the nod angle and velocity, which is a nonlinear term that changes with the change of linear damping due to the duck rotation. One of the references that recently studied the pitch-surge power conversion is reference [18]. Reference [18] models the pitch-surge motions assuming no heave motion; hence there is no effect from the heave motion on the pitch-surge power conversion. The mathematical model used in [18] for the motions in these two DOF is coupled through mass and damping only; there is no coupling in the stiffness. A proportional-Derivative (PD) control is used in [18]; the controller gains are tuned based on a fourth order polynomial in frequency.

Harvesting energy in 3-DOF poses the challenge of developing 3-DOF actuators, wich has a significant impact on the complexity and cost of the system. The pitch and surge motions, however, are usually coupled. This coupling motivates the investigation of shifting the harvested energy between these two coupled modes, aiming at eliminating one actuator of one mode. In other words, due to the coupling, one may design a controller that allows high energy harvesting in one mode while the energy harvesting from the other coupled mode vanishes. This concept is discussed in more detail in this paper in Section VI.

This paper investigates the 3-DOF heave-pitch-surge WEC. A multi-resonant feedback control strategy is developed in this paper that is an extension of the multi resonant control developed for the single DOF heave linear motion in reference [19]. Section II presents the mathematical model of the 3-DOF WEC and highlights the coupling between the pitch and surge modes. Section III discusses the 3-DOF WEC controls problem, and Section IV presents the proposed multi resonant control. Numerical tests on regular, Bretschneider, and Ochi-Hubble waves are presented in Section V. A discussion is presented in Section VI.

II. Mathematical Model

Consider the heave, pitch, and surge degrees-of-freedom of a cylindrical buoy with base radius R, and a mass m. Assuming a body fixed coordinate system located at the buoy's center of gravity. The pitch restoring moment τ_y is:

$$\tau_y = -\rho g V x_{CB} \tag{1}$$

where x_{CB} is the x-coordinate of the center of buoyancy, ρ is the water density, g is the gravitational acceleration, and V is the submerged volume.

Let h be the height of the center of gravity from the base, d_3 is the vertical position of the center of gravity from the mean water level, and θ_5 is the pitch angle, as shown in Fig. 1. The submerged volume is:

$$V = \pi R^2 \left(h + \frac{d_3}{\cos(\theta_5)} \right) \tag{2}$$

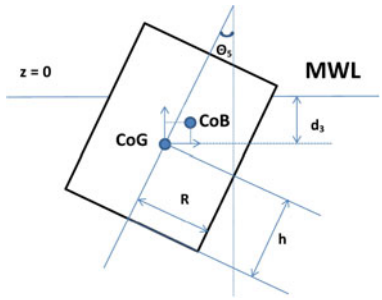

Fig. 1. Geometry of a 3-DoF cylindrical Buoy; MWL is the mean water level, CoG is the Center of Gravity, CoB is the Center of Buoyancy.

The coordinates of the center of buoyancy are:

$$x_{CB} = \frac{\sin(\theta_5)\left(R^2\cos(\theta_5)^2 + R^2 + 4h^2\cos(\theta_5)^2 + 8hd_3\cos(\theta_5) + 4d_3^2\right)}{8\cos(\theta_5)(d_3 + h\cos(\theta_5))} \tag{3}$$

$$z_{CB} = \frac{\left(R^2\cos(\theta_5)^2 - R^2 + 4h^2\cos(\theta_5)^2 + 8hd_3\cos(\theta_5) + 4d_3^2\right)}{8(d_3 + h\cos(\theta_5))} \tag{4}$$

The resulting pitch restoring moment is:

$$\tau_y = -\pi\rho g R^2 \sin(\theta_5)\left(h + \frac{d_3}{cos(\theta_5)}\right) \frac{\left(R^2\cos(\theta_5)^2 + R^2 + 4h^2\cos(\theta_5)^2 + 8hd_3\cos(\theta_5) + 4d_3^2\right)}{8\cos(\theta_5)\left(d_3 + h\cos(\theta_5)\right)} \tag{5}$$

Using a truncated Taylor series expansion, let $sin(\theta_5) = \theta_5 - \theta_5^3/9$ and $cos(\theta_5) = 1 - \theta_5^2/4$, then we can write:

$$\begin{aligned}\tau_y \approx\ & \rho g\pi R^2(\theta_5 - \theta_5^3/9)(h(\theta_5^2 - 1) - d_3)\\ & (4h^2(\theta_5^4/16 - \theta_5^2/2 + 1) +\\ & R^2(\theta_5^4/16 - \theta_5^2/2 + 2) + 4d_3^2 + 8d_3h - 2d_3h\theta_5^2)\\ & /(-(\theta_5^2/4 - 1)(2\theta_5^2 - 8)(h(\theta_5^2/4 - 1) - d_3))\end{aligned}$$

Simplifying the above equation we get:

$$\begin{aligned}\tau_y \approx\ & \rho g\pi R^2(\theta_5 - \theta_5^3/9)\\ & (h^2\theta_5^4/4 - 2\theta_5^2h^2 + 4h^2 + R^2\theta_5^4/16 - R^2\theta_5^2/2 +\\ & 2R^2 + 4d_3^2 + 8d_3h - 2d_3h\theta_5^2)\\ & /(-8(\theta_5^4/16 - \theta_5^2/2 + 1))\end{aligned}$$

Assuming that higher order terms of θ_5 are negligible ($\theta_5^i \approx 0$, $i = 2\cdots 5$), then we get:

$$\tau_y \approx \frac{-\pi\rho g R^2}{4}\left(R^2 + 2h^2 + 4hd_3 + 2d_3^2\right)\theta_5 \tag{6}$$

The heave restoring force F_h is:

$$\begin{aligned}F_h =\ & \rho g\pi R^2\left(\frac{d_3}{\cos(\theta_5)} - d_{30}\right)\\ \approx\ & \rho g\pi R^2\left(d_3\left(1 + \frac{\theta_5^2}{2}\right) - d_{30}\right)\end{aligned} \tag{7}$$

where d_{30} is the vertical position of the center of gravity at equilibrium, for $\theta_5 = 0$.

The system equations of motion are then:

$$\left(m + m_a^{11}\right)\ddot{d}_1 + m_a^{15}\ddot{\theta}_5 + b_1\dot{d}_1 + k_{moor}d_1 = F_e^1 + F_{rad}^1 + u_1 \tag{8}$$

$$\left(m + m_a^{33}\right)\ddot{d}_3 + b_3\dot{d}_3 + \rho g\pi R^2\left(d_3\left(1 + \frac{\theta_5^2}{2}\right) - d_{30}\right) = F_e^3 + F_{rad}^3 + u_3 \tag{9}$$

$$\left(I_5 + I_a^{55}\right)\ddot{\theta}_5 + I_a^{51}\ddot{d}_1 + b_5\dot{\theta}_5 + \frac{\pi\rho g R^2}{4}\left(R^2 + 2h^2 + 4hd_3 + 2d_3^2\right)\theta_5 = F_e^5 + F_{rad}^5 + u_5 \tag{10}$$

where d_1 is the surge displacement, d_3 is the heave displacement, θ_5 is the pitch angular displacement, m_a is added mass, b_i is a friction damping coefficient associated with mode i, k_{moor} is the mooring stiffness coefficient, F_e^i is the excitation force in mode i, F_{rad}^i is the radiation damping force in mode i, and u_i is the control force in mode i. For a regular wave (single frequency), the radiation force can be expressed as two terms: a damping force with a constant damping coefficient and an added mass. Here F_{rad} refers to the radiation damping forces which, for a regular wave, can be computed from the product of the radiation damping coefficients and the velocities as follows:

$$\begin{aligned} F_{rad}^1 &= R_{11}\dot{d}_1 + R_{15}\dot{\theta}_5 \\ F_{rad}^3 &= R_{33}\dot{d}_3 \\ F_{rad}^5 &= R_{51}\dot{d}_1 + R_{55}\dot{\theta}_5 \end{aligned} \tag{11}$$

Substituting the radiation forces above into (8)–(10), and considering (9), If we neglect the higher order term $d_3 \times {\theta_5}^2$, then the heave motion (9) becomes uncoupled from the pitch and surge modes. That is (9) does not have any d_1 or θ_5 terms. Eq. (9) is also linear; that is the heave motion in this 3-DOF WEC problem can actually be solved independently using methods that are designed for heave WEC control such as the method presented in reference [19]. Consider the surge-pitch modes ((8) and (10) after substituting (11) into them), if we assume the higher order terms $d_3 \times \theta_5$ and $d_3^2 \times \theta_5$ are small and negligible, then:

$$\left(m + m_a^{11}\right)\ddot{d}_1 + m_a^{15}\ddot{\theta}_5 + (b_1 - R_{11})\dot{d}_1 - R_{15}\dot{\theta}_5 + k_{moor}d_1 = F_e^1 + u_1 \tag{12}$$

$$\left(I_5 + I_a^{55}\right)\ddot{\theta}_5 + I_a^{51}\ddot{d}_1 + (b_5 - R_{55})\dot{\theta}_5 - R_{51}\dot{d}_1 + K_{22}\theta_5 = F_e^5 + u_5 \tag{13}$$

where

$$k_{22} = \frac{\pi\rho g R^2}{4}\left(R^2 + 2h^2\right) \tag{14}$$

Eqs (12) and (13) are coupled and linear. They can be written in a matrix form. Let the state vector $x = [d_1\,, \theta_5]$; (12) and (13) can be re-written in a state space form as:

$$[M]\ddot{\vec{x}} + [C]\dot{\vec{x}} + [K]\vec{x} = \vec{F}_e + \vec{u} \tag{15}$$

where the state vector $\vec{x} = [d_1\,, \theta_5]^T$, the excitation force vector $\vec{F}_e = [F_e^1\,, F_e^5]^T$, the control force vector $\vec{u} = [u_1\,, u_5]^T$, the matrix $[M]_{2\times 2}$ is:

$$M = \begin{bmatrix} m + m_a^{11} & m_a^{15} \\ I_a^{51} & I_5 + I_a^{55} \end{bmatrix},$$

the matrix $[C]_{2\times 2}$ is:

$$C = \begin{bmatrix} b_1 - h_{11} & -h_{15} \\ -h_{51} & b_5 - h_{55} \end{bmatrix},$$

and the matrix $[K]_{2\times 2}$ is:

$$K = \begin{bmatrix} k_{moor} & 0 \\ 0 & k_{22} \end{bmatrix},$$

where

$$k_{22} = \frac{\pi\rho g R^2}{4}\left(R^2 + 2h^2\right) \tag{16}$$

Thus the pitch-surge system of equations are coupled linear time invariant, and the heave model is an uncoupled linear time invariant equation. This is the dynamic model of a cylindrical WEC. In a similar way, the mathematical model of a spherical buoy can be derived; it is straightforward to show that for a spherical buoy the pitch stiffness and damping are negligible. The heave motion is also decoupled from pitch and surge motions. In the numerical tests section, results for both cylindrical and spherical buoys are presented.

III. The 3-DOF WEC Control Problem

As discussed in Section II, the heave mode is usually decoupled from the pitch and surge modes. Hence the control problem for the heave mode can be solved independently from the pitch and surge modes. The heave control problem is addressed in several references and there are several numerical methods that can be implemented to control the heave motion in an optimal sense in terms of heave energy absorption. So the control of the heave motion will not be addressed in this paper, however, the simulation results will show energy absorption in the heave mode for the purpose of comparison with the energy absorption in the pitch and surge modes. In computing the heave control, a multi-resonant control approach is implemented which is detailed in reference [19] and it is a time domain implementation for the complex conjugate control [20]. Note that for optimal heave energy absorption, the heave motion should be in resonance with the excitation force.

The pitch-surge control problem is a Multi-Input Multi-Output (MIMO) system control where the two inputs are the control force along the surge direction, u_1, and the control moment along the pitch direction, u_5. Both controls are organized in the vector $\vec{u}$ which, from this point in the paper, will refer to these two controls only; the heave control is u_3 and is not included in $\vec{u}$. The outputs of this system $\vec{\eta}$ are the surge position the and pitch angular positions.

The radiation force has two components: the radiation damping force and the added mass force. Both components are

frequency dependant. We start the analysis with the simple case of a regular wave of frequency ω_i; in this case the matrices $[M]$ and $[C]$ in (15) become constant matrices. Then the equation of motion can be written as:

$$\ddot{\vec{x}}_i = -[M_i]^{-1}[K]\vec{x}_i - [M_i]^{-1}[C_i]\dot{\vec{x}}_i + [M_i]^{-1}\left(\vec{F}_{ei} + \vec{u}\right) \tag{17}$$

where the subscript i is added to indicate that this equation is valid for a wave frequency ω_i. If we further consider the WEC problem without the damping and without the external forces terms, we get:

$$\ddot{\vec{x}}_i = -[M_i]^{-1}[K]\vec{x}_i \tag{18}$$

which is an eigenvalue problem. The eigenvalues of the WEC system is determined by the matrix $[M_i]^{-1}[K]$ [21]. These eigenvalues have a very well-defined physical meaning: they contain the square of the angular natural frequencies of the system [21]. For this WEC system we have two eigenvalues.

To harvest the maximum energy from the incoming wave a buoy motion should resonate with the incoming wave; i.e. the natural frequencies need to match that of the incoming wave excitation force. To achieve that, then, the control should change the eigenvalues of the system. Consider a control of the form:

$$\vec{u}_i = -[K_{pi}]\vec{x}_i - [K_{di}]\dot{\vec{x}}_i \tag{19}$$

where each of the $[K_{pi}]$ and the $[K_{di}]$ is a 2×2 controller gain matrix. Substituting this control into Eq. (17), we get:

$$\ddot{\vec{x}}_i = -[M_i]^{-1}\left([K] + [K_{pi}]\right)\vec{x}_i - [M_i]^{-1}\left([C_i] + [K_{di}]\right)\dot{\vec{x}}_i + [M_i]^{-1}\vec{F}_{ei} \tag{20}$$

For this closed loop system, the eigenvalues are computed for the matrix $[M_i]^{-1}\left([K] + [K_{pi}]\right)$; the matrix $[K_{pi}]$ can be designed so that each of the natural frequencies of the closed loop system, ω_{n1} and ω_{n2}, matches the frequency ω_i of the wave excitation force $\vec{F}_{ei}$. That is:

$$\omega_{n1} = \omega_{n2} = \omega_i \tag{21}$$

The natural frequencies for the closed loop system are defined as [22]:

$$\begin{bmatrix} \omega_{n1}^2 & 0 \\ 0 & \omega_{n2}^2 \end{bmatrix} = [M_i]^{-1}([K] + [K_{pi}]) \tag{22}$$

Using (21), (22) can then be used to solve 4 equations in 4 unknowns, the elements of the $[K_{pi}]$ matrix. This completes the design of the proportional part of the controller.

The C3 criteria require that the complex impedance of the controller is equal to the complex conjugate of the WEC mechanical intrinsic impedance; hence the damping of the controller should be equal to the damping of the WEC mechanical intrinsic impedance; or in other words the derivative part of the controller is designed so as to match the damping of the system. Hence, $[K_{di}] = [C_i]$. Substituting into (15):

$$\ddot{\vec{x}}_i = -[M_i]^{-1}\left([K] + [K_{pi}]\right)\vec{x}_i - 2[M_i]^{-1}[C_i]\dot{\vec{x}}_i + [M_i]^{-1}\vec{F}_{ei} \tag{23}$$

The proportional part of the control is designed so as to resonate the system with the excitation force at that frequency, and the derivative part is set to equal the damping in the system. These criteria are the same as the Complex Conjugate Control (C3) criteria; the difference between this control strategy and the C3 is that this control is a time domain implementation, as detailed in Section IV. Hence this control is referred to as Proportional-Derivative Complex Conjugate Control (PDC3). The PDC3 was detailed above for a regular wave. For an irregular wave, Section IV describes the concept of the PDC3. Finally, note that this WEC dynamic system (described by (17)) can be represented by a transfer function, $G_i(s)$, in the Laplace domain as briefed here. For this WEC system, a state vector $\vec{\xi}$ is defined as:

$$\vec{\xi} = [d_1, \theta_5, \dot{d}_1, \dot{\theta}_5]^T \tag{24}$$

Hence, using (17) the state space model can be written as:

$$\dot{\vec{\xi}} = [A_i]\vec{\xi} + [B_i]\left(\vec{F}_{ei} + \vec{u}_i\right) \tag{25}$$

$$\vec{\eta} = [E_i]\vec{\xi} + [D_i]\left(\vec{F}_{ei} + \vec{u}_i\right) \tag{26}$$

where,

The output vector $\eta = [\dot{d}_1, \dot{\theta}_5]^T$, and

$$[A_i] = \begin{bmatrix} [I] & [0] \\ -[M_i]^{-1}[K_i] & -[M_i]^{-1}[C_i] \end{bmatrix}, \tag{27}$$

$[I]$ is a 2×2 identity matrix, and the $[0]$ is a 2×2 zeros matrix.

$$[B_i] = \begin{bmatrix} [0] \\ [M_i]^{-1} \end{bmatrix}, [E_i] = \begin{bmatrix} 0,0,1,0 \\ 0,0,0,1 \end{bmatrix}, [D_i] = \begin{bmatrix} 0 \end{bmatrix}$$

It becomes straightforward to compute the transfer functions matrix if we take the Laplace transform for (25) and (26):

$$s\vec{\chi}(s) = [A_i]\vec{\chi}(s) + [B_i]\left(\vec{F}_{ei}(s) + \vec{U}_i(s)\right) \tag{28}$$

$$\vec{\Upsilon}_i(s) = [E_i]\vec{\chi}(s) + [D_i]\left(\vec{F}_{ei}(s) + \vec{U}_i(s)\right) \tag{29}$$

where $\vec{\chi}(s)$, $\vec{\Upsilon}_i(s)$, $\vec{F}_{ei}(s)$, $\vec{U}_i(s)$ are the Laplace transforms of $\vec{\xi}(t)$, $\vec{\eta}(t)$, $\vec{F}_{ei}(t)$, $\vec{u}_i(t)$, repectively. Solving (28) for $\vec{\chi}(s)$ and substituting into (29) we get:

$$\vec{\Upsilon}_i(s) = \left([E_i]\left(s[I] - [A_i]\right)^{-1}[B_i] + [D_i]\right)\left(\vec{F}_{ei}(s) + \vec{U}_i(s)\right) \tag{30}$$

The transfer function matrix of this WEC system in a regular wave of frequency ω_i is then:

$$G_i(s) = [E_i]\left(s[I] - [A_i]\right)^{-1}[B_i] + [D_i] \tag{31}$$

which, in this case, is a 2×2 matrix that has 4 transfer functions. Fig. 2 shows the block diagram for this WEC control system. This block diagram is a building block in the multi resonant control described in Section IV for irregular waves.

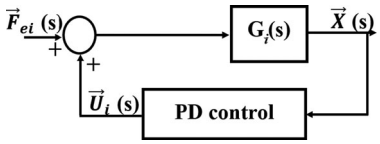

Fig. 2. Block diagram of the WEC control system in a regular wave.

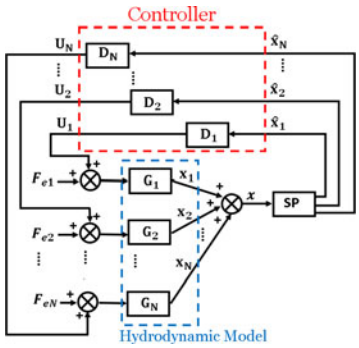

Fig. 3. Block diagram of the WEC multi resonant control system

IV. Multi Resonant Control for 3-DOF WECs

The concept of the multi resonant control is detailed in reference [19] for a 1-DOF linear heave motion. It is here extended to the 2-DOF coupled pitch-surge motion. The strategy of the multi resonant feedback control is to measure the system motion and use these measurements in a feedback control to tune the system's natural frequencies so as to resonate them with the motion frequencies. The excitation force in an irregular wave, however, have many frequencies. As shown in Fig. 3, the measured signals in the vector $\vec{x}$ (in this 2-DOF problem we measure the pitch angular position and surge position) go through a signal processing step (SP block) in which the frequencies, amplitudes, and phases of each of the pitch and surge motions are extracted. The main concept of the multi resonant feedback control is to design a controller for each of these frequencies such that a PDC3 is achieved for that frequency, as detailed below.

The WEC system reacts differently to each exciting frequency (that is radiation damping and added mass depend on the frequency); hence the system dynamics is presented as a series of transfer functions G_i, as shown in Fig. 3. Each G_i represents the dynamics of the WEC in the presence of excitation force F_{ei} of a regular wave with frequency ω_i. Thanks to the linear wave theory, the WEC response to an irregular wave is the collective responses of all the G_i systems, each at its frequency. Note that each G_i is a transfer function matrix that represents a MIMO system identical to the system described in Section III. The calculation of the radiation force in this case is very simple because for each subsystem the radiation force is the radiation damping at that frequency only as in Section III; in other words each subsystem is a regular wave. Hence we can design a PD control $\vec{u}_i$ for each G_i (i.e. for each frequency component of $\vec{x}$) in an optimal sense in a similar way to that described in Section III. The computed controls are then summed to obtain the control $\vec{u}$. Hence, there are N PD controls to be designed for N frequencies in the feedback signal. Note that in order to design each of the N PD controls, the amplitudes and phases of pitch and surge motions, in each individual frequency, are needed to compute the feedback control (see (19)). That is why the SP block extracts these amplitudes and phases for all N frequencies. The feedback control is computed as follows:

$$\vec{u} = \sum_{i=1}^{N} \vec{u}_i = \sum_{i=1}^{N} -[K_{pi}]\vec{x}_i - [K_{di}]\dot{\vec{x}}_i \tag{32}$$

Let the output of the system $\vec{\Upsilon}$ be the vector $\vec{x}$ that includes the pitch angular position and the surge position, then the output can be computed in the Laplace domain as follows:

$$\vec{\Upsilon}(s) = \sum_{i=1}^{N} \vec{\Upsilon}_i(s) = \sum_{i=1}^{N} G_i(s)\left(\vec{F}_{ei}(s) + \vec{U}_i(s)\right) \tag{33}$$

Finally it is worth noting that in implementing this PDC3 control, we do not need to decompose the excitation force $\vec{F}_e$ into its components $\vec{F}_{ei}$. It is decomposed in Fig. 3 only for illustration; in reality the system dynamics takes care of that since each G_i reacts only to the $\vec{F}_{ei}$ component of $\vec{F}_e$.

This implementation of the PD control is novel and is different from previous implementations such as the PD control implementation in reference [18] in which only one PD control is designed to control the system, and a tuning step for the gains is conducted to improve the extracted energy. Hence the PD control in reference [18] is not optimal since it is only one control for all frequencies. On the other hand, in this multi-resonant PD control implementation, there are N PD controllers, each PD controller gains are the optimal gains for their corresponding frequency. Hence, this implementation targets optimal energy harvesting, depending on the accuracy of the signal processing unit. In order to extract the frequencies, amplitudes, and phases of the measured signals, a signal processing step is conducted which is detailed in Section IV-A.

A. Signal Processing

There are several methods that can be used to extract the frequencies, amplitudes, and phases of a dynamic signal. Reference [19] shows the details of using a Fast Fourier Transform for that purpose. In this paper a simple least squares error minimization approach is implemented. The estimate of the measured signal (e.g. estimate of surge motion) is represented as a series expansion as follows:

$$\hat{x}(t) = \sum_{i} A_i \cos(\omega_i t) + B_i \sin(\omega_i t) \tag{34}$$

where the coefficients A_i and B_i are unknown parameters. The A_i and B_i coefficients are computed so as to minimize the summation of the error squares, computed over a period of time (time window). The window size in seconds is fixed and is moving as new estimates are computed. The frequencies ω_i are known since the signal is assumed to have all frequencies listed in a selected vector of discrete frequencies. This optimization problem is relatively simple since the error is a linear function of the coefficients A_i and B_i; these coefficients are then used to compute the magnitude and phase at each frequency in the

selected frequency vector. The accuracy of the estimation depends on the accuracy of the selected frequencies in the frequency vector and on the window size. The higher the number of the frequencies in the selected frequency vector the more accurate of the estimate and the higher is the computational cost. This trade of can be solved via various simulations. Optimal window size can be obtained via simulations as briefed in Section VI.

B. Stability of the Proposed Proportional Derivative Control

The 3-DOF WEC system is decoupled into the 1-DOF heave motion and the 2-DOF pitch-surge motion. Reference [19] details the stability analysis for the 1-DOF heave motion using a multi-resonant PD control. Here the stability of the multi-resonant control of the 2-DOF pitch-surge motion is analyzed.

Consider the block diagram in Fig. 3. There are N controls $D_\imath$, $\imath = 1 \cdots N$. Each controller $D_\imath$ is basically a feedback control for the system $G_\imath$. From the block diagram in Fig. 3, it can be seen that if all the subsystems ($G_\imath$ and $D_\imath$, $\forall \imath = 1 \cdots N$) are stable then the overall system is stable. In other words, if the output from each subsystem is bounded then the linear summation of all the outputs is also bounded. Hence, the stability problem of the system reduces to finding the stability conditions for the subsystem ($G_\imath$ and $D_\imath$) shown in Fig. 2, for arbitrary $\imath$.

To check the stability of each subsystem, substitute from (19) in to (25) and collect terms to get:

$$\dot{\vec{\xi}} = [A_c]\vec{\xi} + [B_c]\left(\vec{F_e}\right) \tag{35}$$

where, the subscript i has been dropped for convenience, the subscript c indicates a closed loop system, and:

$$A_c = \begin{bmatrix} \vec{0} & I \\ -M^{-1}(K + K_p) & -M^{-1}(C + K_d) \end{bmatrix} \tag{36}$$

Recall the definition of K_p and K_d in the multi resonant control in this paper:

$$K_p = M \begin{bmatrix} \omega_{n1}^2 & 0 \\ 0 & \omega_{n2}^2 \end{bmatrix} - K,\ K_d = C \tag{37}$$

Substituting from (37) into (36), we get:

$$A_c = \begin{bmatrix} \vec{0} & I \\ -\begin{bmatrix} \omega_{n1}^2 & 0 \\ 0 & \omega_{n2}^2 \end{bmatrix} & -2M^{-1}C \end{bmatrix} \tag{38}$$

The stability of this closed loop system can be assessed based on the eigenvalues of the matrix $[A_c]$. The eigenvalues of the matrix $[A_c]$ are the roots of the system characteristic equation [23], and hence all eigenvalues need to have non-positive real parts, for a system to be stable. As can be seen from the (38), some terms in the A_c matrix are frequency dependant, hence the eigenvalues of the matrix A_c depends on the frequency. It is possible to compute the eigenvalues symbolically in terms of the elements of the matrix A_c but the expressions for eigenvalues are too long to include in this paper. Rather, it is straight forward to compute the eigenvalues of the matrix A_c numerically, at a large number of different frequencies and verify that all of them are stable. Here, we present one set of eigenvalues computed numerically at $\omega_{n1} = \omega_{n2} = \omega = 4$ rad/s:

$$\lambda_{1,2} = -1.3565 \pm 7.8842i,\ \lambda_{3,4} = -0.2875 \pm 7.9948i$$

which is stable.

It is noted here that this feedback strategy requires measuring the position and velocity of the buoy. Sensors usually introduce noises on the measured signal, and a complete design for the control system should implement techniques to minimize the effect of the sensors noises on the system performance such as the Kalman filer [24]. Noise cancellation, however, is not addressed in this paper.

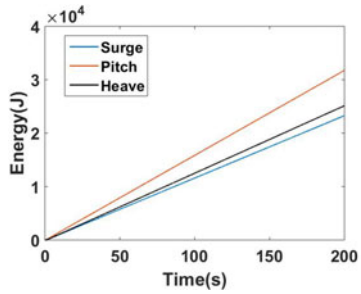

Fig. 4. The harvested energy in heave, pitch and surge modes for a cylindrical buoy in a regular wave.

V. Numerical Tests

The numerical tests presented in this section include cases for a spherical buoy and for a cylindrical buoy. The cylindrical buoy has a radius of 0.8604 m, and a height of 0.7294 m. The mass of the buoy is 858.3987 kg. The spherical buoy has a radius of 0.736 m and a mass of 858 kg. Tests include a regular wave, a Bretschneider wave, and an Ochi-Hubble wave.

A. Cylindrical Buoy in Regular Wave

The cylindrical buoy is tested in a regular wave of amplitude 0.2 m, and a wave period of 1.5708 seconds. Fig. 4 shows the extracted energy in all the three modes. As can be seen in Fig. 4, the energy harvested from the 3-DOF system is slightly higher than three times the energy harvested from only the heave mode.

B. Bretschneider Wave

1) Cylindrical Buoy: Consider a wave with bretschneider spectrum and a significant wave period of 1.5708 seconds, and significant wave height of 1.2 m. The bretschneider spectrum is simulated using 1200 frequencies. The signal processing extracts the most dominant 126 frequencies in the motion and the PDC3 control uses $N = 126$ individual PD controls.

Using the PDC3 control, the energy harvested in heave, surge, and pitch modes is shown in Fig. 5. As can be seen in Fig. 5, the total energy harvested from both pitch and surge motions is 8.545×10^4 Joules, and the energy harvested in the heave mode is 4.4802×10^4 Joules. This means that this 3-DOF buoy harvests about 3 times the energy harvested from the heave mode. The parametric excitation is due to the heave motion

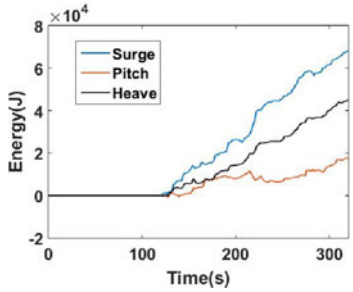

Fig. 5. The harvested energy in heave, pitch and surge modes for a cylindrical buoy. The total energy harvested in the 3-DOF is about 3 times the energy harvested in the heave mode alone.

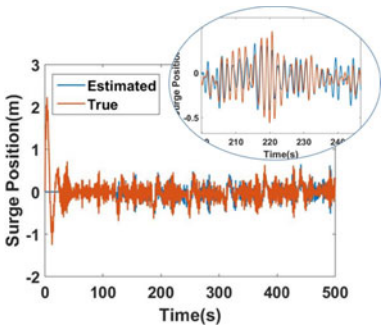

Fig. 6. The surge motion for the cylindrical buoy in a Bretschneider wave.

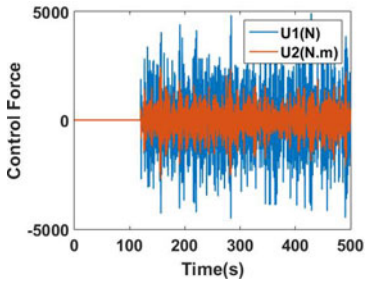

Fig. 7. The control in both the pitch and surge modes.

which, in this test, has an amplitude of 0.3 m most of the time and it reaches to 0.5 m at times. The surge motion amplitude is about 0.25 m as shown in Fig. 6 which shows both the estimated and real surge motions. Fig. 7 shows the control force/torque in both the surge and pitch modes.

2) Spherical Buoy: A bretschneider spectrum is used also here with a significant wave period of 1.5708 seconds, and significant wave height of 1.2 m. The bretschneider spectrum is simulated using 1200 frequencies. The signal processing extracts the most dominant 126 frequencies in the motion and the PDC3 control uses $N = 126$ individual PD controls.

Using the PDC3 control, the energy harvested in heave, surge, and pitch modes is shown in Fig. 8. As expected there is no energy harvested in the pitch direction since for the spherical buoy the pitch damping is almost zero. The energy harvested in the surge mode is about 60% of that harvested in the heave mode.

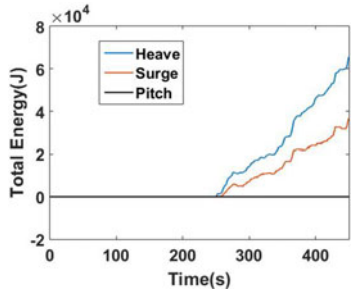

Fig. 8. The harvested energy in heave, pitch and surge modes for a spherical buoy.

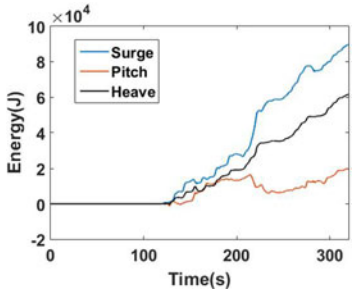

Fig. 9. The harvested energy in heave, pitch and surge modes for a cylindrical buoy in Ochi-Hubble wave.

C. Cylindrical Buoy in Ochi-Hubble Wave

The cylindrical buoy is tested in an Ochi-Hubble wave of significant wave height of 1.2 m. Fig. 9 shows the extracted energy in all the three modes. The heave motion amplitude in this case is within 0.3 m amplitude most of the time; at times it can go up to 0.5 m.

D. Results Validation

In order to validate the performance of the proposed controller, the Capture Width Ratio (CWR) is computed. The Capture Width (CW) is defined as [25]: $CW = p_m/p_w$, where p_m is the mean absorbed power of the buoy in (W), p_w is the wave energy transport in (W/m). The CW is the width of the wave crest of which the energy can be captured by the buoy. The CWR is computed as [26]: $CWR = p_m/Dp_w$, where D is the characteristic dimension of the buoy. The mean absorbed power is already computed in our simulations: $p_m = E_{total}/T_{sim}$. The wave energy transport of regular wave can be computed as:

$$p_w = \frac{1}{2}\rho g \eta^2 c_g \tag{39}$$

Where η is the wave elevation and c_g is the group velocity. For an unidirectional irregular wave, the energy transport can be computed as [27]:

$$p_w = \frac{1}{2}\rho g^2 \int_0^\infty \frac{S(\omega)}{\omega} d\omega \tag{40}$$

Where $S(\omega)$ is the wave spectrum at frequency ω. The characteristic width (D) of the buoys in this paper are selected to be the diameter of the cylinder or sphere [28]. The computed CWR for the buoys in the test cases presented in this paper are:

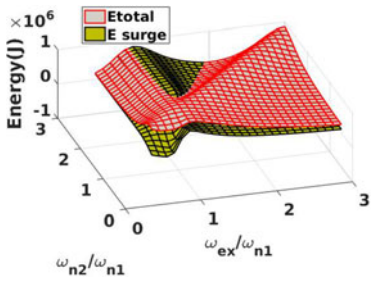

Fig. 10. The total harvested energy (in both pitch and surge) and the harvested energy in surge only for a cylindrical buoy at various design points of the system natural frequencies.

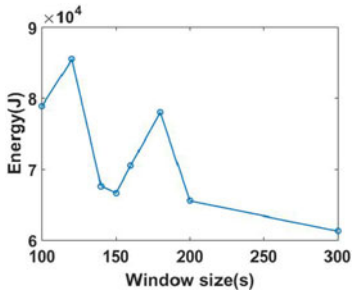

Fig. 11. The moving window size affects the accuracy of the obtained estimation. More accurate estimations result in higher energy harvesting.

0.9511 for the Cylinder buoy in a regular wave, 0.4007 for the Cylinder buoy in a Bretchneider wave, 0.4725 for the Cylinder buoy in a Ochi-Hubble wave, and 0.3761 for the spherical buoy in a Bretchneider wave.

VI. Discussion

The PDC3 presented in this paper targets maximizing the harvested energy assuming the feasibility of harvesting power in both surge and pitch modes. Harvesting power in both modes requires having actuators in each one of them. The PDC3 can be used to shift the energy harvesting from one mode to another, and hence eliminating the need for two actuators. Having only one actuator, while maintaining about the same order of magnitude energy harvesting, has a significant impact in terms of reducing the complexity and cost of the WEC device. To do that, the natural frequencies of the pitch and surge modes will be selected differently from the previous choice presented in (21). Specifically, in (21) the natural frequencies of the pitch and surge modes are selected to resonate with the motion frequency; that selection enables maximum energy harvesting in each of the pitch and surge modes. If the objective is to harvest maximum energy from one mode (e.g. surge) only; then it is better to choose the natural frequencies of the two modes such that most of the energy harvesting is shifted from the pitch to the surge. To find the best selection for the natural frequencies in this case, Fig. 10 is generated which shows how the total harvested energy (from both pitch and surge) varies over a range of selections for the natural frequencies of surge and pitch modes, in a regular wave of height 2.1 m. Fig. 10 also shows how the energy harvested in the surge mode only varies over the same range. Note that, in some regions, the surge energy surface is higher than that of the total energy which indicates that the pitch actuator is actually adding power to the water as opposed to absorbing power. Fig. 10 shows clearly the point of maximum total power, that corresponds to (21), for which the harvested energy comes from both surge and pitch. If we are interested in having no actuator on the pitch mode, then the energy harvesting in the pitch mode should be zero. This condition is satisfied at the lines of intersection between the two surfaces in Fig. 10. So, a candidate selection for the natural frequencies in this case is to consider only the line of intersection between the two surfaces and pick the point of maximum energy on this line. In Fig. 10, the point that corresponds to $\omega_{ex}/\omega_{n1} = 0.9$ and $\omega_{n2}/\omega_{n1} = 3$ is close to that condition; the surge harvested energy at this point is 7.505×10^5 Joules and the total energy (if we have actuators on both pitch and surge) would be 7.61×10^5 Joules.

In the case of a WEC in an irregular wave, there are few parameters that need to be tuned in order to obtain accurate results. One of them is the size of the moving window from which the measurements data are used to extract the frequencies, amplitudes, and phases of the output signals. To tune this parameter, a simulation was conducted on a range of window sizes and the harvested energy, in pitch and surge modes, is plotted versus the window size in Fig. 11 for the cylindrical buoy. The better the estimation of the frequencies, amplitudes and phases the higher the harvested energy since the PDC3 concept is centralized on synchronizing the WEC closed loop system natural frequencies with frequencies of the exciting force. Hence the window size that results in maximum energy harvesting in Fig. 11 is adopted.

This paper assumes a linear hydrodynamic model. The simulator also assumes a linear hydrodynamic model. All modelling errors due to the nonlinear hydrodynamics are not considered in this paper. The model, however, may have uncertainties in some of the parameters, e.g. the stiffness and the mass. Reference [19] presents a numerical analysis conducted on the multi-resonant control of the 1-DOF heave WEC, by allowing the controller to have an error within 5% in each of the mass and the stiffness parameters. The simulator is assumed to have the true values of these parameters. It is shown in [19] that an error within 5% of the stiffness parameter results in an energy drop within 6%. Also, an error within 5% of the mass parameter results in an energy drop within 2%. It is also pointed out here that the controller proposed in this paper is developed based on linear wave theory which is an approximation. In practice, the proposed control might not be optimal due to this approximation.

The PDC3 presented in this paper imposes the C3 criteria; the C3 criteria assumes no constraints on the displacement of the buoy nor the control force limit. In the presence of these constraints, this criteria sometimes result in unrealistic solutions. The case of constrained WEC is not addressed in this study.

The PD control adopted in this paper computes the derivative of the position signal which is assumed measured using a position sensor. The derivative operation itself is non-causal, and its approximations add high frequency noise. In the simulations conducted in this paper, however, the errors are not significant because of the relatively slow motion of the WEC compared to the sampling rate. Another way of reducing derivative errors is to use a low pass filter. The focus of this paper is to present

the concept of the control without details on the implementation issues.

Finally, this paper demonstrated a control strategy that amplifies the energy harvesting by a factor of 3 when using a 3-DOF compared to the 1-DOF WEC. It is noted here that some studies have shown theoretically that it is possible to get this factor of 3 (see e.g. reference [29]), without discussing the controller that will actually achieve this amplification factor. This paper is a demonstration for one controller that can achieve that.

VII. Conclusion

For three-degree-of-freedom surge-heave-pitch wave energy converters, and using a linear dynamic model, it is possible to show that the energy capture would be in the order of three times the energy capture of a heave-only WEC; depending on the buoy shape and control method used. This paper presented a novel time domain feedback control strategy that is optimal based on the criteria of the complex conjugate control, and demonstrates achieving the factor of three for the 3-DOF WEC compared to the 1-DOF WEC. The multi resonant control presented in this paper can also be used to shift the harvested energy from one of the coupled modes to another, enabling the elimination of one of the actuators needed in a 3-DOF wave energy converter. This feedback control strategy does not require wave prediction; it only requires the measurement of the buoy position and velocity.

References

[1] U. A. Korde, "On control approaches for efficient primary energy conversion in irregular waves," in *Proc. OCEANS Conf.*, Sep. 1998, vol. 3, pp. 1427–1431.

[2] U. A. Korde, M. P. Schoen, and F. Lin, "Time domain control of a single mode wave energy device," in *Proc. 11th Int. Offshore Polar Eng. Conf.*, Stavanger, Norway, 2001, pp. 555–560.

[3] F. Fusco and J. Ringwood, "Hierarchical robust control of oscillating wave energy converters with uncertain dynamics," *IEEE Trans. Sustain. Energy*, vol. 5, no. 3, pp. 958–966, Jul. 2014.

[4] J. Ringwood, G. Bacelli, and F. Fusco, "Energy-maximizing control of wave-energy converters: The development of control system technology to optimize their operation," *IEEE Control Syst.*, vol. 34, no. 5, pp. 30–55, Oct. 2014.

[5] J. Scruggs, S. Lattanzio, A. Taflanidis, and I. Cassidy, "Optimal causal control of a wave energy converter in a random sea," *Appl. Ocean Res*, vol. 42, pp. 1–15, 2013. [Online]. Available: http://www.sciencedirect.com/science/article/pii/S0141118713000205

[6] D. G. Wilson *et al.*, "A comparison of WEC control strategies," Sandia Nat. Lab., Albuquerque, NM, USA, Tech. Rep. SAND 2016–4293, May 2016.

[7] A. Babarit, G. Duclos, and A. H. Clment, "Comparison of latching control strategies for a heaving wave energy device in random sea," *Appl. Ocean Res.*, vol. 26, pp. 227–238, Jul. 2004.

[8] J. Henriques, M. Lopes, R. Gomes, L. Gato, and A. Falco, "On the annual wave energy absorption by two-body heaving {WECs} with latching control," *Renewable Energy*, vol. 45, pp. 31–40, 2012. [Online]. Available: http://www.sciencedirect.com/science/article/pii/S0960148112001322

[9] J. Falnes, *Ocean Waves and Oscillating Systems—Linear Interactions Including Wave-Energy Extraction*. Cambridge, U.K.: Cambridge Univ. Press, 2002, ch. 4.

[10] U. Korde, R. Robinett, and D. G. Wilson, "Approaching maximum power conversion with exergy-based adaptive wave-by-wave control of a wave energy converter," in *Proc. MTS/IEEE OCEANS*, Genova, Italy, 2015, May 18–21.

[11] U. A. Korde, "Up-wave surface elevation for smooth hydrodynamic control of wave energy conversion in irregular waves," in *Proc. IEEE OCEANS*, Sand Diego, CA, USA, 2013. [Online]. Available: ftp://128.171.151.230/bhowe/outgoing/IEEEOES_2013/papers/130424-002.pdf.

[12] J. Falnes, "Wave-energy conversion through relative motion between two single-mode oscillating bodies," *J. Offshore Mech. Arctic Eng*. vol. 121, no. 1, pp. 32–38, Feb. 1999. [Online]. Available: http://link.aip.org/link/?JOM/121/32/1

[13] A. F. Davis, J. Thomson, T. R. Mundon, and B. C. Fabien, "Modeling and analysis of a multi degree of freedom point absorber wave energy converter," in *Proc. ASME 2014 33rd Int. Conf. Ocean, Offshore Arctic Eng.*, San Francisco, CA, USA, Jun. 8–13, 2014, Paper OMAE 2014–23475.

[14] D. V. Evans, "A theory for wave-power absorption by oscillating bodies," *J. Fluid Mech.*, vol. pp. 1–25, Sep. 1976. [Online]. Available: http://journals.cambridge.org/article_S0022112076001109

[15] D. Evans, "Some theoretical aspects of three-dimensional wave-energy absorbers," in *Proc. 1st Symp. Wave Energy Utilization*, Chalmers Univ. Technol., Gothenburg, Sweden, 1979, pp. 77–106.

[16] M. J. French and R. H. Bracewell, "P.S. frog a point-absorber wave energy converter working in a pitch/surge mode," in *Proc. 5th Int. Conf. Energy Options, Role Alternatives World Energy Scene*, Univ. Reading, Reading, Berkshire, U.K., 1987.

[17] H. Young and J. Pollock, "Variable coefficient control of a wave-energy device," Univ. Edinburgh, Edinburgh, U.K., Tech. Rep., 1985. [Online]. Available: http://www.homepages.ed.ac.uk/v1ewaveg/0-Archive/EWPP%20archive/1985%20EWPP%20Variable%20coefficient%20control%20of%20a%20wave%20energy%20device.pdf

[18] H. Yavuz, "On control of a pitching and surging wave energy converter," *Int. J. Green Energy* . vol. 8, no. 5, pp. 555–584, 2011. [Online]. Available: http://dx.doi.org/10.1080/15435075.2011.576291

[19] J. Song, O. Abdelkhalik, R. Robinett, G. Bacelli, D. Wilson, and U. Korde, "Multi-resonant feedback control of heave wave energy converters," *Ocean Eng.*, vol. 127, pp. 269–278, 2016. [Online]. Available: http://www.sciencedirect.com/science/article/pii/S0029801816304346

[20] J. Falnes, "A review of wave-energy extraction," *Mar. Struct.* vol. 20, no. 4, pp. 185–201, Oct. 2007. [Online]. Available: http://www.sciencedirect.com/science/article/pii/S0951833907000482

[21] G. Takács and B. Rohal'-Ilkiv. *Basics of Vibration Dynamics*. London, U.K.: Springer-Verlag, 2012, pp. 25–64. [Online]. Available: http://dx.doi.org/10.1007/978-1-4471-2333-0_2

[22] W. Palm, *Mechanical Vibration*. New York, NY, USA: Wiley, 2007. [Online]. Available: https://books.google.com/books?id=GZJRAAAAMAAJ

[23] K. Ogata, *Modern Control Engineering*, 4th ed. Upper Saddle River, NJ, USA: Prentice-Hall, 2001.

[24] J. L. Crassidis and J. L. Junkins, *Optimal Estimation of Dynamic Systems*. Boca Raton, FL, USA: CRC Press, 2004.

[25] K. Budar and J. Falnes, "A resonant point absorber of ocean-wave power," *Nature*, vol. 256, pp. 478–479, 1975.

[26] A. Babarit, "A database of capture width ratio of wave energy converters," *Renewable Energy*, vol. 80, pp. 610–628, 2015.

[27] Ø. Y. Rogne, "Numerical and experimental investigation of a hinged 5-body wave energy converter," Ph.D. dissertation, Dept. Petroleum Eng., Norway, Univ. Sci. Technol., 2014.

[28] A. Pecher, *Performance Evaluation of Wave Energy Converters*. Denmark, The Netherlands: River Publishers, 2012.

[29] J. Falnes, *Ocean Waves and Oscillating Systems—Linear Interactions Including Wave-Energy Extraction*. Cambridge, U.K.: Cambridge Univ. Press, 2002. [Online]. Available: http://app.knovel.com/hotlink/toc/id:kpOWOSLII8/ocean-waves-oscillating/ocean-waves-oscillating

Ossama Abdelkhalik received the B.S. and M.S. degrees in aerospace engineering from Cairo University, Cairo, Egypt, and the Ph.D. degree in aerospace engineering from Texas A&M University, College Station, TX, USA. He is an Associate Professor at Michigan Tech University, Houghton, MI, USA. His research interests include global optimization, dynamics, and optimal control with applications to the space trajectory optimization and wave energy conversion optimal control.

Shangyan Zou received the Bachelor's degree in mechanical engineering from Nanjing Forestry University, Nanjing, China. He is currently working toward the Ph.D. degree in the Department of Mechanical Engineering and Engineering Mechanics, Michigan Technological University, Houghton, MI, USA. His research interest includes control and optimization of wave energy converters.

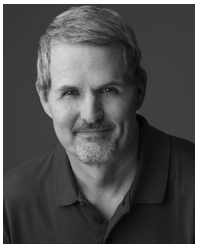

Rush D. Robinett III received the B.S. and Ph.D. degrees from Texas A&M University, College Station, TX, USA, and the M.S. degree from the University of Texas at Austin, Austin, TX, USA, all in aerospace engineering. He is the Co-Director of the Agile and Interconnected Microgrids Center, the Director of Research, and the Richard and Elizabeth Henes Chair Professor in mechanical engineering-engineering mechanics at Michigan Technological University, Houghton, MI, USA. In January 2013, he retired from Sandia National Laboratories after 25 years of service as the Senior Manager of the Grid Modernization and Military Energy Systems Group focusing on the research and development of microgrids and networked microgrids. During his 25 year career, he worked on ballistic missile defense, spacecraft systems, glide weapons, teams of robots, and renewable energy grid integration. He has authored more than 150 technical articles, including three books and holds eleven patents. He is an Associate Fellow of AIAA.

Giorgio Bacelli received the Laurea Magistrale degree in electronic engineering from the Universit Politecnica delle Marche, Ancona, Italy, in 2006, and the Ph.D. degree in electronic engineering from the Center for Ocean Energy Research, Maynooth University, Maynooth, Ireland, in 2014. He is currently with Sandia National Laboratories, Albuquerque, NM, USA, working on the design and implementation of control strategies for wave energy converters.

David G. Wilson (M'95–SM'17) received the B.S. and M.S. degrees from Washington State University, Pullman, WA, USA, and the Ph.D. degree from the University of New Mexico, Albuquerque, NM, USA, all in mechanical engineering. He is an R&D Controls Engineer in the Department of Electrical Science and Experiments, Sandia National Laboratories, Albuquerque, NM, USA. He has over 25 years of R&D engineering experience in energy systems, robotics, automation, and space and defense projects. He has published more than 75 technical articles, three books, and four patents. His research interests include nonlinear/adaptive control, distributed decentralized control, and energy/entropy control for nonlinear dynamical systems. He is currently developing Hamiltonian surface shaping and power flow control for critical energy surety infrastructures and renewables for microgrids, wave energy systems, and wind farms. He is a Senior member of AIAA.

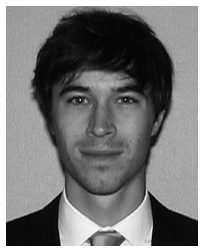

Ryan Coe received the B.S. degree in ocean engineering in 2009, and the Ph.D. degree in aerospace engineering in 2013, both from Virginia Tech, Blacksburg, VA, USA. He is currently a Senior Research Engineer in the Water Power Technologies Department, Sandia National Laboratories, Albuquerque, NM, USA. His research interests include hydrodynamic modeling, wave tank testing, and wave energy converter design and dynamics.

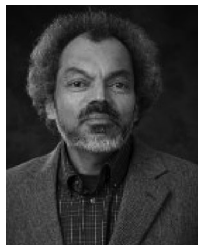

Umesh Korde has worked on many aspects of wave energy conversion for over three decades, more recently focusing on hydrodynamic control of oscillating bodies and pressure distributions. He serves as associate editor for the journal *J. Ocean Engineering and Marine Energy (Springer)* and is a fellow of the American Society of Mechanical Engineers.